Integrated Supply- and Demand-Side Energy Management for Expeditionary Environmental Control

E. M. Craparo[a,*], J. G. Sprague[b]

[a]*Naval Postgraduate School, 1411 Cunningham Road, Monterey, CA, 93943 USA*
[b]*US Navy, Stuttgart, DE*

Abstract

This paper examines efficiencies achieved by optimal scheduling of power generation equipment and electrical loads in a hybrid smart micro-grid under conditions where load activity may be delayed or advanced with negligible impact to system performance. We model military expeditionary energy systems to analyze the performance of existing unmanaged components and estimate potential savings obtained by coordinated management of battlefield heating and cooling systems. We employ rolling horizon optimization models to examine performance under varying degrees of uncertainty about future load demand and renewable production.

We propose a novel mechanism to reduce power production costs through optimal prescriptive scheduling of loads, reducing peak demand and generator peak-to-average power ratios and facilitating a persistent shift to higher fuel efficiencies. In contrast to existing methods that employ either supply-side or demand-side management, we propose intelligently coordinating both sides to achieve greater efficiency. Using sensitivity analysis, this paper quantitatively demonstrates hows grid composition, temperature band tolerance, and energy storage capabilities contribute to fuel efficiency under this approach.

Keywords: `Load management, smart grids, optimal scheduling, expeditionary power, generators`

1. Introduction

The Department of Defense (DOD) is the largest energy consumer within the U.S. government, accounting for 80% of all federal consumption [1]. Operational energy [1] demands for fiscal year (FY) 2015 were estimated at 96.2 million barrels of refined petroleum products, or more than 263,000 barrels per day [4].

Globally, aircraft account for an estimated 75% of this usage, with ships, ground vehicles, and support operations consuming the remaining 25% [5]. This mix changes in active combat zones, where large cargo aircraft are less likely to be refueled on the ground, up-armored tactical ground vehicles are heavier and less fuel-efficient, and a greater portion of electricity is supplied by local generation rather than a municipal grid. A 2009 United States Marine Corps (USMC) study of 5.2 million gallons of fuel consumed by Marine Expeditionary Battalion - Afghanistan (MEB-A) discovered that 32% of the fuel usage was devoted to electrical power generation [6].

The majority of this generated electricity is used for environmental control. Analysis of USMC systems found air conditioners and environmental control units (ECUs) accounted for 57% of expeditionary power demand [7]. Similarly, research conducted over a 48-hour period on an instrumented expeditionary camp at Fort Blevins showed that 97.7% of total electricity consumption was devoted to maintaining desirable temperatures in occupied areas [8]. In a 2012 survey of multiple studies, the Congressional Research Service cited a range of 57% to 70% of generator power output committed to expeditionary environmental control [1]. This paper adopts a value of 60% for further analysis.

1.1. The Cost of Heating and Cooling

Operational energy costs and risks have been the subject of Congressional hearings, contributed to the creation of a presidentially-appointed Assistant Secretary of Defense for Operational Energy Plans and Programs, and received more than $4 billion to support demand reduction and supply diversification efforts [9, 10].

1.1.1. Monetary Costs

In FY2007, the Army Petroleum Center purchased 590 million gallons of fuel to supply U.S. forces operating in Iraq and Afghanistan [11]. Applying USMC estimates that

---

*Corresponding author
Email address: `emcrapar@nps.edu` (E. M. Craparo)

[1]Operational energy is defined in U.S. law as "the energy required for training, moving, and sustaining military forces and weapons platforms for military operations. The term includes energy used by tactical power systems and generators and weapons platforms" [2]. This is distinct from facility energy, described by [3] as the energy to power fixed installations, enduring locations, and non-tactical vehicles (NTVs).

32% of this fuel was directed to electrical power generation, and that 60% of the resulting electricity was utilized for environmental control, we estimate that nearly 20% of the 2007 fuel requirement, or 113 million gallons, were devoted to heating and cooling. Additionally, contractor activities—including prime power generation for U.S. forces—require substantial fuel whose cost is embedded in the contract price rather than in DOD consumption figures, resulting in underestimation of actual operational fuel requirements [1].

Security, transportation, storage, and distribution expenses escalate the cost of fuel consumed in combat zones to between \$3 to \$45 per gallon if delivered by land and \$29 to \$45 per gallon if delivered by air [1]. In particular, the U.S. Army Environmental Policy Institute calculated that the fully burdened cost of fuel in Iraq during 2008 is \$14.13 per gallon. Applying this figure to our annual requirement of 113 million gallons produces an estimated cost of \$1.6 billion for battlefield heating and cooling in FY2007 alone [12].

1.1.2. Human Costs

Resupply convoys are an inviting target and significant operational vulnerability, and logistic convoy personnel account for many of the killed and wounded in recent conflicts. Applying 2007 convoy casualty factors of one casualty per 3.762 million gallons of delivered fuel in Iraq and per 2.329 million gallons of fuel delivered in Afghanistan, 33 killed or wounded personnel in a single year are attributable to the demand for heating and cooling [11].

1.2. Efficiency and Availability Trade-off

Cyclical loads such as ECUs present a unique and significant obstacle to achieving maximum efficiency in an expeditionary energy system. Though frequently idle and drawing little power, the defining characteristic of these loads is that they *could* activate at any moment. Thermostats monitoring temperature within each facility issue control signals to associated ECUs without regard to existing or pending demands upon the grid. We label these loads, which act in ways that are locally appropriate but globally naïve, as *unmanaged*. Their demand-side autonomy requires the grid to maintain sufficient online capacity to support unilateral load decisions or risk an overload condition. As a result of these design choices, the system suffers from chronic overgeneration, underutilization, and suboptimal fuel efficiency.

1.2.1. Peak and Average Loads

Design guidance specifies a 1.0 demand factor for air conditioning loads, indicating that an appropriately designed power system must be capable of immediately meeting the full, simultaneous demands of all connected units [13].[2] Actual ECU duty cycles depend on factors such as

Figure 1: Simulated 30 kW generator operation with loads at 75% and 25% duty cycles.

structure characteristics and current environmental conditions, and are often well below 1.0 [14].

Simulation results for generator output with connected loads operating at 75% and 25% duty cycles are presented in Fig. 1 to illustrate the relationship between ECU duty cycle and generator loading. When connected loads operate at 75% duty cycle, average power demand is 21.6 kilowatt (kW) and peak demand is 28.8 kW. Generator utilization is high, and unused capacity (indicated by white space) is low. At 25% duty cycle, average power demand is only 7.2 kW while peak demand remains 28.8 kW. Utilization is much lower, substantial capacity is wasted, and the generator frequently runs below 30% load, leading to inefficient and potentially damaging operation [15]. Observations in the field have repeatedly observed this effect [16, 15]. Fig. 2 displays actual generator load at a camp in Afghanistan over 96 hours in June 2012.

These demand peaks establish the minimum amount of power that the generation network must constantly be

---

[2]Other demand factors include laundry (0.8), base operations (0.7), communications (0.7), billeting (1.0), latrines (0.8), warehouse (0.6), and kitchen facilities (0.9) [13].
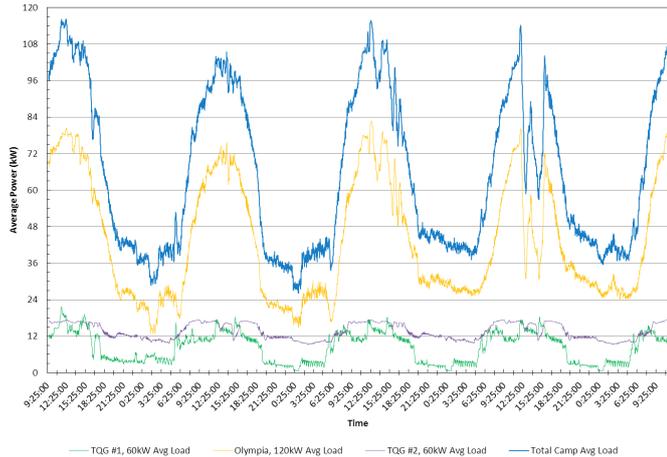
Figure 2: U.S. Forces Afghanistan camp electrical demand over a 96-hour period in June 2012. Three generators and site cumulative are displayed, from [16]

Figure 3: Fuel efficiency of U.S. military TQGs as a function of generator size and load factor, from [15].

prepared to deliver. Failure to have sufficient online capacity may overload generators, causing voltage and frequency instability that can damage sensitive equipment or trip protective circuits and immediately disconnect serviced loads. [3] Though a generator may, on the average, be capable of powering additional devices, the brief periods of peak demand from those loads already being serviced prevent the connection of any further equipment.

1.2.2. Generator Fuel Efficiency

Generator efficiency (η) is the fraction of chemical energy from fuel that is converted to usable electrical energy [15]. Efficiency is generally greater for larger units and rises non-linearly with load factor for all sizes of generators. Fig. 3 depicts the relationship between load factor and fuel efficiency for five sizes of U.S. military Tactical Quiet Generators (TQGs).

System efficiency is maximized by selecting the smallest generator capable of providing the required power. For example, a single 40 kW load is better served by a 60 kW generator operating at 0.67 load factor ($\eta \approx 32\%$) than a 200 kW generator running at 0.20 load factor ($\eta \approx 25\%$).

The present requirement to size generators based on peak, rather than average, power demand leads us to provision high-capacity generators from which we tolerate substantial periods of inefficient, low power operation as the price to be paid for peak readiness.

---

[3]Note that military specification generators may operate reliably up to 150% of rated power for limited periods under certain conditions [17]. Unless explicitly specified, this paper adopts nameplate ratings as the upper limit of generator capacity for two reasons. First, the robustness of military generators is an operational risk mitigator reserved for the benefit of those in the field. Second, many generators used in combat theaters are not military specification and offer no assurance of similar overload capacity.
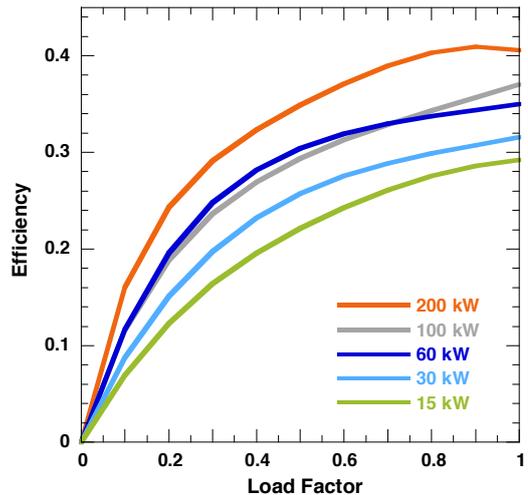
1.3. Contributions

This paper proposes a novel mechanism in which time-shiftable, non-critical electrical loads in an expeditionary energy grid are optimally scheduled to minimize fuel consumption. We combine information on current load and generator status, generator fuel efficiencies, and shelter conditions and characteristics in a mixed integer linear program (MILP) that prescriptively defines operational schedules. We construct scenarios with perfect future knowledge to establish optimal upper bounds on improvements to fuel efficiencies, and use simulation of unmanaged systems to establish our lower bounds. Finally, we employ rolling-horizon optimization to determine how a fielded system might perform relative to these bounds. Our approach exploits non-linear fuel efficiency curves, the ability to advance or delay the operation of certain loads, and knowledge of energy storage and renewable production to reduce the number of running generators and ensure the remaining generators operate in their most fuel efficient range. To our knowledge, no other work has considered the potential efficiencies to be gained by optimally coordinating generators and loads in an expeditionary setting.

2. Literature Review

Our work has connections to three fields of research and application. The first field involves efforts, led by the U.S. military and supported by industry and academia, to improve the efficiency of fielded generators, ECUs, and structures through engineering and procedural solutions. This field plays a critical role that is largely complementary to our own research efforts, rather than directly related. Thus, we refer the reader to [18] for a review of the literature in this area. The second area involves hybrid microgrid architectures incorporating renewable production,

uncertain demand, and energy storage for use in remote military and civil applications. We provide a review of the literature in this field, as well as the related but distinct field of deferrable electric load management in commercial and residential scenarios.

2.1. Hybrid Smart Microgrids

For clarity, we begin by articulating the features and characteristics that distinguish micro, hybrid, and smart grids.

Microgrids combine multiple potentially dissimilar generation sources with various loads through a network of controllers, distribution panels, and cabling [19]. Properly designed microgrids save fuel by aggregating numerous small loads for servicing with a fewer number of larger, more efficient power sources. In one example, the United States Army (USA) observed fuel savings of 17% by replacing thirteen 60 kW TQGs at Bagram Airfield, Afghanistan with a one megawatt (MW) microgrid in August 2011 [9].

Hybrid power systems combine two or more dissimilar energy sources into a single composite source intended to provide greater efficiency or increased resilience over single-source generation systems [15]. Components of an expeditionary hybrid system may include reciprocating diesel generators, photovoltaic (PV) solar arrays, wind turbines, and battery storage.

Smart grids utilize information about energy sources, loads, and storage devices to improve grid efficiency and reliability [20]. This basic information can be augmented with additional data on user behavior, environmental conditions, or forecasts to enhance renewable integration and make predictive management decisions.

Existing microgrid optimization literature focuses on minimizing costs via long-term infrastructure investment or short-term supply-side dispatch decisions. Bouaicha *et al.* [21] examine minimum-cost fulfillment of specified demand by incorporating estimates of near-term renewable generation forecasts. Ulmer [22] extends this work by maximizing the endurance of an isolated grid at a fixed location by using renewable generation estimates to inform capital planning decisions. Ongoing work by Newman [23] focuses on development of a decision support tool to aid in pre-deployment equipment provisioning selections to minimize DOD total mission lifecycle costs. Sadiqi *et al.* [24] conduct similar analysis for rural community electric hybrid power systems in Afghanistan.

2.2. Demand-Side Management

Load-following electrical grids treat energy demands of connected loads as immutable parameters that must be completely satisfied if the grid is to remain stable. Generator output will vary, storage devices will charge and discharge, and additional production resources will be brought online or placed offline to match supply to demand.

Introducing basic smart grid features permits demand side management (DSM), a feedback and control mechanism to reshape the demand profile to match available supply. DSM implementations vary by provider, customer, and connected load. The least intrusive solutions merely notify consumers of an opportunity to reduce costs by limiting demand, while the most prescriptive programs allow the grid to explicitly permit or deny operation of a particular device [25]. Candidate loads for DSM control must be *time-shiftable*, or capable of being satisfied within a range of time periods, and *cyclical*, or naturally subject to alternating on/off periods.[4] Substantial research has been performed on the application of DSM to electric vehicle (EV) charging and to commercial and residential appliance control, and various DSM approaches have been successfully implemented to reduce costs and manage peak demand.

2.2.1. Appliance Control

Prescriptive residential and commercial DSM constitutes a bargain between energy suppliers and customers in which customers surrender a degree of control over the timing of demand satisfaction in exchange for lower utility rates or other incentives. Suppliers exert this control to stabilize demand across multiple customers during peak periods. The ability to level demand reduces the risk of overloading portions of the grid, permits increased renewable penetration, and potentially reduces the amount of spinning reserve[5] that a utility must maintain [25].

Loads most suitable for shifting include heating, ventilation, and air conditioning (HVAC), water heating, clothes and dish washing appliances, and EV charging. Vlot *et al.* [27] find that 12% of Dutch national electricity usage is suitable for residential load shifting, and that investment in a nationwide smart grid would have the effect of adding 700 MW of generation and 5 gigawatt-hours (GWhs) of storage to the grid with a cost recovery period of less than seven years. In their stochastic optimization of energy bidding strategies in community microgrids, Nguyen and Le [28] show that flexible HVAC scheduling can significantly reduce costs while enabling increased renewable participation. Similarly, Tarasak *et al.* [29] show that a notional hotel participating in a demand bidding program[6] can more than double peak monetary rewards by scheduling HVAC loads. In more recent work, Jiang *et al.* [31] consider various optimal control methods for controlling

---

[4] *Deferrable* is commonly used in the literature to describe loads that may be delayed to a more advantageous time. We adopt the convention that *time-shiftable* loads include not only deferrable loads, but also those demands that may be fulfilled earlier.

[5] Spinning reserve is unused production capacity available to compensate for dramatic load changes or generation outages. It is online, synchronized to the grid, and capable of reaching full power within 10 minutes [26].

[6] Demand bidding programs are utility-managed programs that encourage large customers to commit to future demand reductions if called upon by the utility during peak periods. See [30] for details of one program.

the heating, ventilation and air-conditioning systems in a building, while Wu *et al.* [32] employ a combination of optimal control and model predictive control. Zachar and Daoutidis [33] employ a hierarchical control framework for heating and cooling, using stochastic optimization for long-term planning and deterministic optimization for short-term planning.

Barriers to adoption of DSM include capital investment costs for grid integration, lack of standardized communication and negotiation protocols between sources, loads, and storage, and undeveloped cost and reward sharing arrangements between energy suppliers and customers [25], [34], [35]. The DOD has begun limited work to establish communications protocols through the Hybrid Intelligent Power (HI-Power) and Alternative Energy Demonstration Project [36], [37]. Further protocol development and implementation was a top recommendation of the 2014 Massachusetts Institute of Technology (MIT) Lincoln Laboratory study [15].

2.3. Simultaneous Supply- and Demand-Side Management

The works described in Section 2.1 focus mainly on supply side management, i.e., optimally producing energy so as to minimize cost while satisfying demand. Those in Section 2.2 utilize demand-side management, which shifts or adapts loads appropriately based on the available supply. In contrast, we propose coordinating supplies and demands in order to optimize the overall system performance. While some work appears in the literature on simultaneous supply- and demand-side management [38], it appears less frequently than single-side management techniques due to the fact that in many applications, no central authority exercises influence over both the supply and demand sides. Expeditionary heating and cooling thus presents a somewhat unusual opportunity for greater fuel savings than could be achieved through supply- or demand-side management alone. Moreover, to our knowledge, no prior work explicitly models the efficiency curves of expeditionary generators in order to achieve fuel savings.

3. Expeditionary Energy Systems

We limit our examination to tactical power only, excluding prime and commercial power production and distribution. Prime power is utility-grade power support for major bases and airfields using generators larger than 200 kW and with output voltages up to 4,160 volts (V), while tactical power generation ranges from 0.5 kW to 200 kW and is "generated by a mobile electrical-power unit dedicated to supporting the missions of units engaged in combat operations" [39].

In practice, electrical generation and distribution at expeditionary locations is often accomplished by an ad-hoc arrangement of available equipment assembled over the months or years that a site has been in operation [16], [37], [40], [41], [42], [43]. Grid topology may be the result of the most expedient courses of action rather than
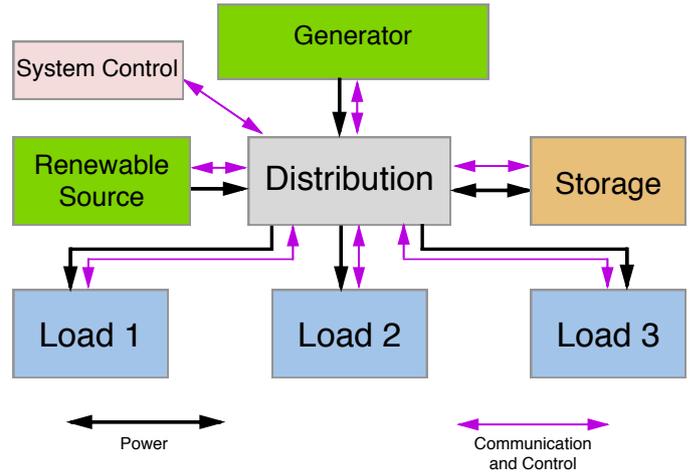
Figure 4: Notional smart grid configuration. The control node monitors conditions and adjusts loads and sources to maximize efficiency.

the most effective or efficient. High priority loads such as tactical operations centers (TOCs) or medical treatment areas are frequently assigned a dedicated generator in an attempt to increase reliability at those locations. Energy system architectures used in practice include spot generation configurations, multiple-generator configurations, hybrid systems, and smart grids. A detailed description of these frameworks appears in [18].

Optimized time-shiftable load management as envisioned in our research requires a minimum foundation of smart grid capabilities that include ECU and generator control, as well as environmental monitoring of shelters serviced by the ECUs. Fig. 4 represents a smart hybrid grid with bidirectional communication and control channels that permit each node to broadcast current status, send or receive commands, and signal upcoming events. Existing or developmental systems that provide a limited subset of smart grid capabilities include the Improved Power Distribution System, Electrical (IPDISE) and the DRASH Intelligent Power Technology family of equipment [44], [45]. These solutions focus almost exclusively on supply-side management by offering generator control, supply consolidation, and phase balancing. With the exception of load shedding, they do not offer DSM capabilities.

3.1. Energy Production

We focus our study on diesel generators, which are widely used and consume substantial amounts of fuel. Other energy production sources such as wind and photovoltaic solar are described in [18].

Reciprocating diesel generators provide a robust, reliable source of tactical power in sizes from 5 kW to 200 kW. The Advanced Medium Mobile Power Sources (AMMPS) series of medium tactical generators supply tactical power requirements from 5 kW to 60 kW across the DOD. More significant power requirements are currently met by the 100 kW and 200 kW TQGs, pending fielding of the Large

Advanced Mobile Power Sources (LAMPS) under a design and build contract awarded in 2012 [44].

Once started, generators require a warm-up period before they are ready to synchronize phase with previously running generators and assume their share of electrical load. Likewise, when a generator is to be secured it must be electrically unloaded and permitted to cool before shutting down. Thus, our model enforces required generator run\rest times.

3.2. Energy Storage

Intermittent sources such as wind and solar require an energy storage device to bridge periods of low production. Diesel generator systems, with or without the inclusion of renewable production, also exhibit increased efficiency when energy storage capabilities are present and intelligently managed.

Storage mechanisms used in the power industry include chemical batteries, flywheels, compressed air, pumped hydroelectric, and others [46]. Complexity, size, weight, initial investment, or specialized site requirements render all but batteries unsuitable for the tactical environment [19]. Lithium-ion is presently the most common chemistry due to its high power capability, high power to weight and volume ratios, and reasonable lifecycle [19].

Batteries are direct current (DC) devices; interfacing with alternating current (AC) generators requires an appropriate conversion. On charging, a rectifier converts the AC output of the generator into a DC source that can charge the battery. On discharge, an inverter converts DC energy from the battery into AC power to supplant or assist the generator in powering AC loads. This rectification/inversion process, combined with losses in charging circuitry and battery chemistry, result in round-trip energy efficiencies well below 100%. In practice, only about 80% of the energy devoted to charging a battery will be recovered during discharge [15]. For simplicity, this paper considers a notional storage device with charge and discharge rate limits that are constant over the entire range of the storage level, and we assume that the battery level varies linearly with the chosen charge and discharge rates.

3.3. Electrical Loads

We broadly characterize expeditionary power loads as *stable* or *transient* based upon the fluctuations that they create in the grid. Stable loads are relatively small or exhibit little short-term variation. Examples are lighting, communication systems, computer networks, and aggregated minor plug loads. Transient loads are cyclical and large in proportion to overall demand. They may operate either semi-autonomously, such as HVAC, refrigeration, and water heating, or under the control of a user, such as kitchen, laundry, or water purification equipment.

Figure 5: 36,000 BTU/hr environmental control unit (left). ECUs externally installed in support of insulated fabric tents (right), from [48] and [49].

3.3.1. Environmental Control Units

ECUs are electrically powered, thermostatically controlled devices employed to heat, cool, dehumidify, filter, and circulate air in expeditionary shelters [47]. ECUs are rated by their capacity, measured in British thermal unit (BTU)/hr, to add (heating mode) or remove (cooling mode) thermal energy from a shelter. Higher thermal capacity units require greater amounts of electrical power. Some ECU models offer low and high heat settings, and all provide a fan-only setting. During cooling mode, however, it is significant to note that an ECU is not capable of variable output. It either operates at full capacity—and full power—or it provides no cooling at all.[7] Fig. 5 shows a typical ECU, as well as a set of ECUs deployed in the field.

3.3.2. Expeditionary Shelters

Expeditionary shelters accommodate operations centers, billeting, medical suites, dining and recreation facilities, aircraft and vehicle maintenance, communication centers, and other functions. Desirable characteristics of a shelter include speed and ease of erection, durability in adverse environments, and low weight and volume for portability. Many shelters in the DOD inventory are soft-wall, consisting of fabric walls, floor, and roof supported by a metal or airbeam frame [47], [50], [51], [52]. These shelters are shipped unassembled and erected on site.

Standard fabric shelters are poorly insulated, necessitating substantial HVAC capacity to maintain desired internal temperature in extreme climates. Modifications to improve insulative value and reduce HVAC demands include solar shades, insulating liners, and spray-on foam insulation [37], [53]. Other factors influencing heating and cooling requirements for each shelter include the contents, location, and physical characteristics of the shelter.

3.4. Distribution

Distribution equipment includes power distribution panels and cabling required for assembly of a grid that can

---

[7]Temperature control on many ECUs is managed by using a refrigerant bypass valve to unload, rather than stop, the compressor once the low temperature setpoint is reached. The compressor and fan continue to run during this "off" cycle but consume far less power.

safely and reliably deliver power from the point of production to the point of consumption.

The tactical power distribution system of record within the USMC is titled the Mobile Electric Power Distribution-Replacement (MEPDIS-R), while the USA and United States Air Force (USAF) family of equipment is named the Power Distribution Illumination System, Electrical (PDISE) [54, 55]. Both systems incorporate protective devices and provide the ability to connect multiple generators.

Having established the foundational understanding of expeditionary energy systems, we continue with a discussion of our model limitations, assumptions, and mathematical formulation.

4. Model

Our model minimizes fuel consumption by defining an optimal schedule for operating generators, utilizing ECUs, and managing an energy storage device. The principal constraint is maintaining internal structure temperature within acceptable upper and lower bounds.

4.1. Model Simplifications and Assumptions

We adopt various simplifications and assumptions to maintain computational tractability, overcome shortfalls in available data, and maintain focus on our primary research questions:

Loads are balanced. Total load in each period is split among all operating generators proportional to their nameplate rated capacity. Single phase loads are connected and operated such that all phases are adequately balanced. We presume that an architecture capable of achieving the optimal control we describe is also capable of balancing loads and phases, and therefore this simplification does not diminish the validity of our conclusions.

Energy storage. Charge and discharge rate limits are constant over the entire range of battery level, and battery level varies linearly with chosen charge and discharge rates.

Power distribution. We do not model limitations and constraints of specific distribution systems. All power production in each period is aggregated and available to any load.

Thermal behavior. We estimate shelter and ECU performance under varying environmental conditions using software tools rather than field or test data. Air density (ρ) and heat capacity (cp) vary less than 4% within the temperature range considered by this model. We treat these as constants with the specified values.

Generator fuel consumption curve. Generator fuel consumption is modeled as piecewise linear using six points from 0 to 100% of rated power. This reflects a limitation in source data gathered under testing protocols that required evaluation only at these discrete power levels [56].

4.2. Optimization Formulation

This section describes a discrete-time mixed integer linear program designed to minimize generator fuel consumption by prescribing periods of ECU operation subject to specified internal temperature requirements and equipment operating limitations.

4.2.1. Sets and Indices

$s \in S$	Set of all structures and associated ECUs
$g \in G$	Set of generators
$t \in T$	Set of time intervals
$c \in C$	Set of fuel curve linearization points
$b \in B$	Set of storage batteries

4.2.2. Parameters

cp	Heat capacity of air [0.9526 $BTU/kg \cdot C$]
ρ	Density of air [1.1894 kg/m^3]
w	Time interval width [minutes]
ϕ	Proportion of heat flow that manifests as a change in air temperature
v_s	Internal volume of structure s [m^3]
$\beta_{s,t}$	Equilibrium heat transfer rate intercept for structure s in interval t [BTU/hr]
$m_{s,t}$	Equilibrium heat transfer rate slope for structure s in interval t [$BTU/hr \cdot^\circ C$]
$\dot{Q}_s^-$	Heat removal capacity of ECU for structure s [BTU/hr]
r_s	Power required by ECU s in operation [kW]
k_g	Maximum rated power of generator g [kW]
$hi_{s,t}$	High temperature limit for structure s in interval t [$^\circ C$]
$lo_{s,t}$	Low temperature limit for structure s in interval t [$^\circ C$]
$erun_s$	Minimum run time for ECU s [minutes]
$grun_g$	Minimum run time for generator g [minutes]
$erest_s$	Minimum rest time for ECU s [minutes]
$grest_g$	Minimum rest time for generator g [minutes]
w	Time interval width [minutes]
u_t	Unmanaged load requirements in time interval t [kW]
a_t	Unmanaged power production in time interval t [kW]
$fint_g$	Y-intercept of fuel curve for generator g [galllons/hr]
$fx_{g,c}$	Fuel curve x-axis linearization points [fraction of full power]
$fy_{g,c}$	Fuel curve y-axis linearization points [gallons/hr]
min_b	Minimum acceptable charge level battery b [kWh]
cap_b	Capacity of battery b [kWh]
$charg_b$	Maximum charge rate of battery b [kW]
$disch_b$	Maximum discharge rate of battery b [kW]
η_b	Efficiency of battery b [%]

4.2.3. Continuous Variables

$\tau_{s,t}$	Shelter s internal temp at end of interval t [$^\circ C$]
$f_{g,t}$	Total fuel consumed by generator g during interval t [gallons]
$vf_{g,t}$	Power-dependent fuel consumption rate by generator g during interval t [gallons/hr]
$blvl_{b,t}$	Level of battery b at end of interval t [kWh]
P_t^*	Power level of running generators in interval t [fraction of full power]
$Pg_{,t}$	Power level of generator g in interval t [fraction of full power]
	$= \begin{cases} P_t^* & \text{if generator } g \text{ is running in interval } t \\ 0 & \text{otherwise} \end{cases}$
$in_{b,t}$	Power directed to battery b in interval t [kW]
$out_{b,t}$	Power supplied by battery b in interval t [kW]

4.2.4. Binary Variables

$Genon_{g,t} =$	$\begin{cases} 1 & \text{if generator } g \text{ is running during interval } t \\ 0 & \text{otherwise} \end{cases}$
$Genstart_{g,t} =$	$\begin{cases} 1 & \text{if generator } g \text{ starts at the beginning of interval } t \\ 0 & \text{otherwise} \end{cases}$
$Genstop_{g,t} =$	$\begin{cases} 1 & \text{if generator } g \text{ stops at the beginning of interval } t \\ 0 & \text{otherwise} \end{cases}$
$Y_{s,t} =$	$\begin{cases} 1 & \text{if ECU for shelter } s \text{ operates during time interval } t \\ 0 & \text{otherwise} \end{cases}$
$Thermstart_{s,t} =$	$\begin{cases} 1 & \text{if shelter } s \text{ ECU starts at the beginning of time interval } t \\ 0 & \text{otherwise} \end{cases}$
$Thermstop_{s,t} =$	$\begin{cases} 1 & \text{if shelter } s \text{ ECU stops at the beginning of time interval } t \\ 0 & \text{otherwise} \end{cases}$

4.2.5. Specially Ordered Set Type 2 (SOS2) Variables

$\lambda_{g,t,c}$	weight of cth fuel curve linearization inflection point for generator g in interval t

Linear interpolation of fuel consumption is performed by employing specially ordered set, type 2 (SOS2) variables in the General Algebraic Modeling System (GAMS)

optimization software. SOS2 variable sets can be of any length, however the values assigned to members of the set must obey two rules: (1) at most two members of the set may have non-zero values, and (2) any non-zero values must be adjacent members of the set.

4.2.6. Objective

$$minimize \sum_{t \in T} \sum_{g \in G} f_{g,t} \tag{1}$$

Our formulation minimizes total fuel consumption subject to the following:

4.2.7. Constraints

$$\sum_{s \in S} Y_{s,t} r_s + u_t + \sum_{b \in B} in_{b,t} \leq \sum_{g \in G} P_{g,t} k_g + \sum_{b \in B} \eta_b out_{b,t} + a_t \quad \forall t \in T \tag{2}$$

$$P_{g,t} \leq Genon_{g,t} \forall g \in G, t \in T \tag{3}$$

$$P_{g,t} \geq P_t^* - (1 - Genon_{g,t}) \forall g \in G, t \in T \tag{4}$$

$$P_{g,t} \leq P_t^* \forall g \in G, t \in T \tag{5}$$

$$P_{g,t} = \sum_{c \in C} \lambda_{g,t,c} fx_{g,c} \forall g \in G, t \in T \tag{6}$$

$$vf_{g,t} = \sum_{c \in C} \lambda_{g,t,c} fy_{g,c} \forall g \in G, t \in T \tag{7}$$

$$\sum_{c \in C} \lambda_{g,t,c} = 1 \forall g \in G, t \in T \tag{8}$$

$$\lambda_{g,t,c} \geq 0 \forall c \in C, g \in G, t \in T \tag{9}$$

$$f_{g,t} = \frac{w}{60}(fint_g Genon_{g,t} + vf_{g,t}) \forall g \in G, t \in T \tag{10}$$

$$lo_{s,t} \leq \tau_{s,t} \leq hi_{s,t} \forall s \in S, t \in T \tag{11}$$

$$\tau_{s,t} = \tau_{s,t-1} + \frac{w}{60} \cdot \frac{\phi}{\rho \cdot v_s \cdot cp} \left(m_{s,t} \cdot \tau_{s,t-1} + \beta_{s,t} - \dot{Q}_s^- Y_{s,t} \right)$$
$$\forall s \in S, t \in T \tag{12}$$

$$Y_{s,t} = Y_{s,t-1} + Thermstart_{s,t} - Thermstop_{s,t} \quad \forall s \in S, t \in T \tag{13}$$

$$Y_{s,t'} \geq Thermstart_{s,t} \forall s \in S, t \leq t' < t + erun_s/w \tag{14}$$

$$Y_{s,t'} \leq (1 - Thermstop_{s,t}) \forall s \in S, t \leq t' < t + erest_s/w \tag{15}$$

$$Thermstart_{s,t} + Y_{s,t-1} \leq 1 \forall s \in S, t \in T \tag{16}$$

$$Thermstop_{s,t} - Y_{s,t-1} \leq 0 \forall s \in S, t \in T \tag{17}$$

$$Thermstart_{s,t} + Thermstop_{s,t} \leq 1 \forall s \in S, t \in T \tag{18}$$

$$Genon_{g,t} = Genon_{g,t-1} + Genstart_{g,t} - Genstop_{g,t} \forall g \in G, t \in T \tag{19}$$

$$Genon_{g,t'} \geq Genstart_{g,t} \forall g \in G, t \leq t' < t + grun_g/w \tag{20}$$

$$Genon_{g,t'} \leq (1 - Genstop_{g,t}) \forall g \in G, t \leq t' < t + grest_g/w \tag{21}$$

$$Genstart_{g,t} + Genon_{g,t-1} \leq 1 \forall g \in G, t \in T \tag{22}$$

$$Genstop_{g,t} - Genon_{g,t-1} \leq 0 \forall g \in G, t \in T \tag{23}$$

$$Genstart_{g,t} + Genstop_{g,t} \leq 1 \forall g \in G, t \in T \tag{24}$$

$$in_{b,t} \leq charg_b \forall b \in B, t \in T \tag{25}$$

$$out_{b,t} \leq disch_b \forall b \in B, t \in T \tag{26}$$

$$blvl_{b,t} = blvl_{b,t-1} + \frac{w}{60}(in_{b,t} - out_{b,t}) \forall b \in B, t \in T \tag{27}$$

$$min_b \leq blvl_{b,t} \leq cap_b \forall b \in B, t \in T \tag{28}$$

$$P_t^* \geq 0 \forall t \in T \tag{29}$$

$$P_{g,t} \geq 0 \forall g \in G, t \in T \tag{30}$$

9

$$vf_{g,t} \geq 0 \forall g \in G, t \in T \qquad (31)$$

$$Genstart_{g,t} \in \{0,1\} \forall g \in G, t \in T \qquad (32)$$

$$Genstop_{g,t} \in \{0,1\} \forall g \in G, t \in T \qquad (33)$$

$$Genon_{g,t} \in \{0,1\} \forall g \in G, t \in T \qquad (34)$$

$$Thermstart_{s,t} \in \{0,1\} \forall s \in S, t \in T \qquad (35)$$

$$Thermstop_{s,t} \in \{0,1\} \forall s \in S, t \in T \qquad (36)$$

$$Y_{s,t} \in \{0,1\} \forall g \in G, t \in T \qquad (37)$$

Equation (2) ensures that power supplied by all sources in each period is sufficient for all running loads.

Equations (3) through (5) require all paralleled generators to operate at the same percentage of full load.

Equations (6) through (9) calculate variable fuel consumption by each generator as a piecewise linear function of operating state and power level. Recall that for each generator g and time step t, we have $\lambda_{g,t,c} > 0$ for at most two adjacent values of c. Thus, the fuel used is calculated as a convex combination of the fuel used at the two relevant inflection points. Equation (10) determines the fuel consumed by each generator in each time period.

Equation (11) maintains the temperature of each structure within the specified range.

Equations (12) through (18) establish ECU and shelter thermal continuity in successive periods and enforce minimum run and rest times for each ECU. Equation (12) is the primary expression of our thermal model; further details of this model are available in [18].

Equations (19) through (24) establish generator continuity in successive periods and enforce minimum run and rest times for each generator.

Equations (25) through (28) maintain battery charge level continuity and enforce battery charge and discharge limitations.

Equations (29) through (37) enforce binary and non-negativity constraints.

5. Application and Analysis

The thermal and optimization models are combined with a discrete-time simulation to develop an ensemble framework that accepts equipment characteristics, environmental factors, projected unmanaged demand, and anticipated renewable production as inputs and returns operating schedules for ECUs, generators, and storage as outputs. Fig. 6 depicts this relationship.
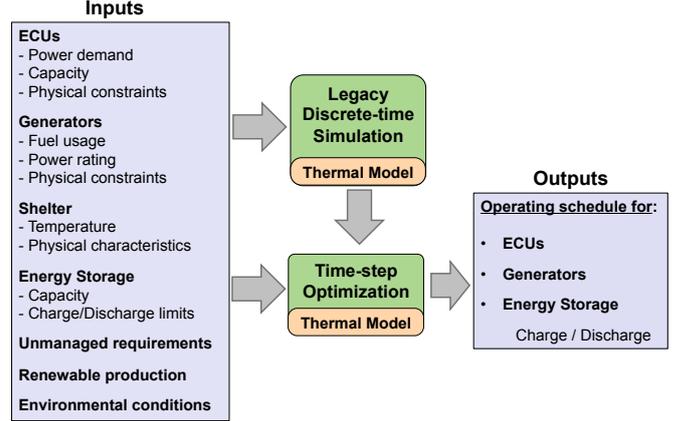
Figure 6: Ensemble simulation and optimization model framework.

5.1. Model Variants

We develop six variants of the optimization model to evaluate the potential impact of optimal load management. The first implementation performs only discrete-time simulation of a legacy unmanaged grid to establish a minimum fuel efficiency benchmark. Another model, granted complete visibility on upcoming conditions and permitted to optimize all decisions, establishes a theoretical upper bound on fuel efficiency under ideal circumstances. Four intermediate variants aid in isolating the contribution of load management and evaluating potential system performance under imperfect knowledge. The six variants are:

Legacy unmanaged (LGCY). We stipulate that all generators run continuously to ensure sufficient power is available to supply all connected loads and perform time-step simulation to establish thermostatically-determined ECU start and stop times. The model sums total ECU and unmanaged loads in each period to determine total demand, and supplies this demand first with perishable renewable production and then with generator output to fulfill any remaining balance. Equations (6) through (10) determine generator fuel consumption based on load in each period.

Perfect future knowledge, storage only management (PFK-SOM). A hybrid policy in which ECUs are unmanaged and thermostatically controlled as in the legacy unmanaged arrangement and generators run continuously. We optimize storage charge and discharge using full visibility over the entire planning period.

Perfect future knowledge, generator and storage management (PFK-GSM). ECUs remain unmanaged and thermostatically controlled as in PFK-SOM. We optimize generators operation *and* energy storage using full horizon visibility.

Perfect future knowledge, full management (PFK-FM). We provide the optimization model of Section 4.2

10

visibility on all parameters in every period throughout the planning horizon, allowing it to return globally optimal decisions for ECU operation, generator control, and storage management. To maintain computational tractability we use the linear relaxation of this integer model unless otherwise specified.

Rolling horizon, perfect future knowledge (RH-PFK).
We divide the entire planning horizon into multiple increments and iterate through them sequentially. At the beginning of iteration n the model receives perfect knowledge of conditions upcoming in time increments n and $n+1$, where each increment contains one or more discrete time steps. The model then develops an optimal schedule for these two increments. Increment n decision variables for generators ($Genon_{g,t}, Genstart_{g,t}, Genstop_{g,t}$) and ECUs ($Y_{s,t}$) are fixed to the value determined by the schedule, and the model finishes by executing increment n to determine optimal levels for the variables that were not fixed. This cycle of two-increment visibility/optimization and one-increment execution continues until the end of the planning horizon. [57] describes this approach in more detail.

Rolling horizon with uncertainty (RH-U). Similar to RH-LPK, however at the beginning of increment n we supply the model with *forecasted* demand and environmental parameters for increments n and $n+1$ and receive an optimal ECU, generator, and storage management schedule for these increments based on our forecasts. In the execution phase we replace the increment n forecasted planning parameters with "actual" values drawn from specified random distributions and optimize for this single increment.

The first four variants demonstrate the effect of increasing optimization opportunities over the full horizon. The final two variants evaluate rolling horizon performance under both perfect and imperfect knowledge conditions. Table 1 provides a summary of all six model variants.

5.2. Uncertainty Implementation
The two-step rolling horizon variants require *forecasted* demand and environmental conditions for the planning phase, and specification of *actual* demand and environmental conditions for the execution phase. We define these parameters as follows:

$a_t^{forecast}$ — Forecasted renewable production in period t

a_t^{actual} — Actual renewable production in period t

$u_t^{forecast}$ — Forecasted unmanaged demand production in period t

u_t^{actual} — Actual unmanaged demand in period t

$\beta_{s,t}^{forecast}$ — Forecasted thermal intercept for shelter s in period t

$\beta_{s,t}^{actual}$ — Actual thermal intercept for shelter s in period t

Table 1: Summary of model variations.

Variant		ECUs	Storage	Generators
Legacy	LGCY	Fixed to simulation results		Fixed ON
Storage optimized with perfect future knowledge	PFK-SOM	Fixed to simulation results	Optimized	Fixed ON
Generator and storage optimized with perfect future knowledge	PFK-GSM	Fixed to simulation results	Optimized	Optimized
Perfect future knowledge, full management	PFK-FM	Optimized	Optimized	Optimized
Rolling horizon with perfect future knowledge	RH-PFK	Optimized	Optimized	Optimized
Rolling horizon with uncertainty	RH-U	Optimized	Optimized	Optimized

For the rolling horizon with perfect future knowledge (RH-PFK) variant, all actual values equal their respective forecasted values.

For rolling horizon with uncertainty (RH-U), actual values for the execution phase are random uniform values, $U[min, max]$, centered around forecasted values with a floor of zero to prevent negative results. We introduce three parameters to specify the maximum absolute difference between forecasted and actual values:

var_a — Renewable production variability

var_u — Unmanaged demand variability

var_β — Thermal intercept variability

$$a_t^{actual} = max \left(0, U \left[\left(a_t^{forecast} - var_a \cdot a_t^{forecast}\right), \right.\right.$$
$$\left.\left. \left(a_t^{forecast} + var_a \cdot a_t^{forecast}\right)\right]\right) \tag{38}$$

$$u_t^{actual} = max \left(0, U \left[\left(u_t^{forecast} - var_u \cdot u_t^{forecast}\right), \right.\right.$$
$$\left.\left. \left(u_t^{forecast} + var_u \cdot u_t^{forecast}\right)\right]\right) \tag{39}$$

$$\beta_{s,t}^{actual} = max \left(0, U \left[\left(\beta_{s,t}^{forecast} - var_\beta \cdot \beta_{s,t}^{forecast}\right), \right.\right.$$
$$\left.\left. \left(\beta_{s,t}^{forecast} + var_\beta \cdot \beta_{s,t}^{forecast}\right)\right]\right) \tag{40}$$

Conditions may exist where actual unmanaged demand in a period is higher than forecasted, while actual renewable production is simultaneously lower than forecasted, leading to infeasibilities from Equation (2). We prevent

this by requiring the RH-U model to provision sufficient power generation capacity in the planning stage to accommodate demand and renewable variability.

Additionally, actual environmental conditions may differ from forecasted values, causing shelter temperatures to exceed our upper or lower bounds during the execution phase. Rather than enforcing Equation (11) in the RH-U model, we examine the extent and frequency of temperature violations as a measure of effectiveness, alongside fuel consumption.

6. Baseline Grid Configuration

We first implement our model variants on an initial baseline grid configuration, then perturb certain grid parameters in order to perform a sensitivity analysis. Our initial configuration is based on a tactical power system surveyed by Shields and Newell [58] in September and October 2011. Located in southwest Afghanistan, at the time of the survey this power system supplied a patrol base that housed 45 Marines sheltered in eight structures served by ten ECUs, three conventional generators, and two hybridized generators with battery storage.

The hybrid components of the system include a 84 kWh storage battery de-rated to 42 kWh and a 4.8 kW PV system that harvested approximately 25 kWh of solar energy per day [59]. Combat operations center (COC) and billeting plug loads averaged 68.5 kWh per day, and two 2.5 kW B0075 refrigerated storage units and a Ground Based Operation Surveillance System (GBOSS) consumed another 61.7 kWh per day [58].

6.1. Equipment Manifest

Our baseline configuration approximates the grid assessed by Shields and Newell, with some slight modifications outlined in [18]. Tables 2 through 4 provide parameters for the shelters and generators included in the baseline model configuration. Additional information on thermal model slope and intercept calculations are available in [18].

6.2. Storage, Renewables, Unmanaged Demand, and Uncertainty

We establish the following parameters for the baseline configuration:

Storage: All storage is aggregated into a single battery type with the following characteristics:

$$charg_b = disch_b = \frac{0.2 \cdot cap_b}{hr} = 8.4 \text{ kW} \qquad \forall b \in B$$

(41)

$$\eta_b = 75\% \qquad \forall b \in B \qquad (42)$$

In other words, a battery can charge or discharge 20% of its capacity each hour, and its efficiency is 75% [15].

Table 2: Initial shelter configurations.

Shelter Configurations				
Parameter	Shelters 1-5	Shelters 6, 7	Shelter 8	Shelter 9
Usage	Billeting	Billeting	Billeting	COC
Type	Base-X 305	Base-X 305	Base-X 307	Base-X 307
Min. internal temp. [$^\circ F$]	70	70	70	70
Max. internal temp. [$^\circ F$]	80	80	80	80
ECU capacity [BTU/hr]	36,000	20,000	60,000	96,000
ECU power [kW]	4.5	1.6	8.5	13.0
Thermal slope [$BTU/(hr \cdot^\circ C)$]	-931	-931	-1,226	-1,254
Thermal intercept [BTU/hr]	37,790	37,790	48,794	60,456
ECU run/rest time [$minutes$]	2/2	2/2	2/2	2/2

Table 3: Initial generator configurations.

Generator Configurations				
Parameter	Gen 1	Gen 2	Gen 3	Gen 4
Type	AMMPS	AMMPS	AMMPS	AMMPS
Frequency [$Hertz$]	60	60	60	60
Rating [kW]	10	10	30	60
Gen. run/rest time [$minutes$]	5/5	5/5	5/5	5/5

Table 4: Fuel consumption of AMMPS generator sets, from [56].

Generator Fuel Consumption					
% Power	Fuel Consumption by model [gal/hr]				
	5 kW	10 kW	15 kW	30 kW	60 kW
110	0.55	0.98	1.39	3.11	5.33
100	0.51	0.88	1.24	2.79	4.92
75	0.42	0.70	0.95	2.00	3.96
50	0.34	0.53	0.73	1.39	2.74
25	0.27	0.38	0.49	0.92	1.66
10	0.23	0.29	0.38	0.65	1.08
0	0.20	0.24	0.31	0.59	0.74

Renewables: For simplicity, renewable production of 25 kWh per day is evenly distributed for a forecasted

renewable contribution of 1.04 kW in each period.

$$a_t = a_t^{forecast} = 1.04 \text{ kW} \qquad \forall t \in T \qquad (43)$$

This forecast could easily be improved by utilizing a typical insolation curve for the location in question; we anticipate that such a forecast would improve our model's performance.

Unmanaged demand: We treat COC and billeting plug loads of 68.5 kWh per day as evenly distributed over the 24-hour day, resulting in a power demand of $\frac{68.5\text{kWh}}{24\text{h}}$ =2.85 kW during each period. The potential demand of two 2.5 kW refrigeration units are added to establish a forecasted unmanaged demand level of 7.85 kW in each period.

$$u_t = u_t^{forecast} = 7.85 \text{ kW} \qquad \forall t \in T \qquad (44)$$

Again, this forecast could be improved with the use of empirical data.

Uncertainty: We specify maximum renewable and thermal intercept variability for Equations (38) through (40) as:

$$var_a = var_u = 0.15 \qquad (45)$$
$$var_\beta = 0.05 \qquad (46)$$

To accommodate this uncertainty we require that the RH-U variant provision generator capacity that is at least 120% of forecasted demand for each period.

7. Baseline Configuration Results

This section presents the results obtained from running all six model variants on multiple initial conditions using the baseline grid configuration over an optimization horizon of ten working hours, divided into two-minute time steps ($w = 2$). Rolling horizon variants (RH-PFK and RH-U) employed 20 iterations, planning for 60 minutes and executing 30 minutes in each iteration. Optimization dimensions and computational performance data appear in the appendix.

7.1. Fuel Consumption

Cumulative fuel consumption for each model variant over the ten-hour optimization horizon is tabulated in Table 5. Unsurprisingly, the legacy unmanaged (LGCY) mode is at the upper end of fuel consumption. Though we expect the performance of perfect future knowledge, storage-only management (PFK-SOM) to be at least equal to that of LGCY, our results indicate that the best integer solution for PFK-SOM uses slightly more fuel. This is attributable to our stopping conditions that include a relative optimality gap of 4%. We conclude that a PFK-SOM scheme in which generators are always running offers no

Table 5: Cumulative fuel consumption for the baseline grid configuration after 10 hours.

Baseline Cumulative Fuel Consumption			
Variant	Best Solution [gallons]	Best Possible [gallons]	Reduction vs. LGCY [%]
PFK-GSM	23.5	23.1	28.6
PFK-SOM	33.0	32.8	NA
LGCY	32.9	32.9	NA
PFK-FM (RMIP)	15.9	NA	51.7
PFK-FM (integer)	22.3	19.7	32.2
RH-PFK	22.9	22.9	30.4
RH-U	23.7	23.5	28.0

significant advantage over existing LGCY methods for the modeled grid conditions.

The perfect future knowledge, generator and storage management (PFK-GSM) performance shows a considerable reduction in fuel consumption relative to LGCY values. Recall that in PFK-GSM the generators and storage are optimized and ECU operation is fixed beforehand to the behavior that would occur if they were under thermostatic control. These results indicate that under some conditions we may see considerable improvements to fuel efficiency by merely predicting—and subsequently constraining—upcoming ECU behavior and then optimizing generator operation to match the defined load schedule.

The RH-U model, burdened with our requirement to provision sufficient capacity to meet 120% of predicted load in each period, nevertheless consumes only 3.5% more fuel than its perfect knowledge counterpart, RH-PFK. This is explained by the high system load factor for both variants, illustrated in Fig. 7. As Fig. 3 indicates, generator efficiency "flattens" as load factor increases, resulting in only modest changes to fuel efficiency between load factors above 50%. The LGCY variant operates well below a 50% load factor and suffers markedly impaired efficiency as a consequence.

7.2. Thermal Observations

Fig. 8 displays the interior temperature of Base-X 305 shelter equipped with a B0014 ECU over the ten-hour horizon for LGCY and RH-U variants. The sawtooth pattern shown by LGCY is characteristic of a thermostatically controlled load that switches modes only when reaching a high or low limit. PFK-SOM and PFK-GSM fix ECU operation to the same thermostatically determined cycles and exhibit the exact same behavior.

The optimal ECU scheduling of RH-U results in temperature variations driven by globally optimal fuel efficiency considerations. RH-PFK presents similar results
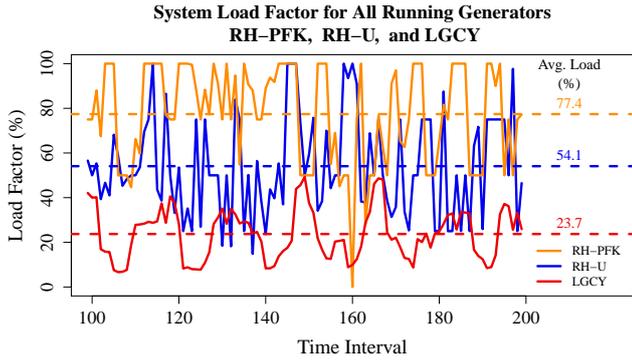
Figure 7: Generator loading for the RH-PFK, RH-U, and LGCY model variants in the baseline grid configuration.

Figure 8: Thermal behavior of a Base-X 305 shelter equipped with a B0014 ECU under LGCY and RH-U variants in the baseline grid configuration.
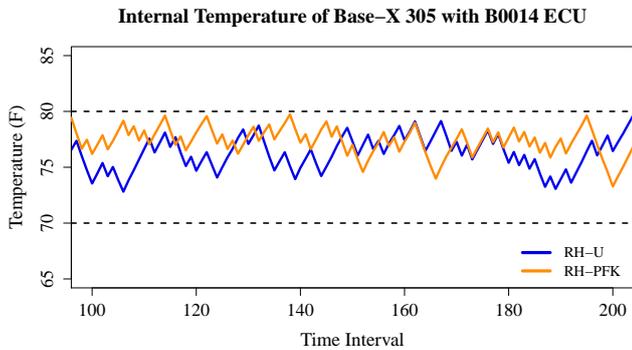
Figure 9: Comparison of interior temperatures for Base-X 305 shelter with B0014 ECUs under RH-U and RH-PFK.

to RH-U; Fig. 9 displays both over a subset of the optimization period for comparison.

The direct current air conditioner (DCAC) units have far less cooling capacity than the B0014 ECU, resulting in slower cooling and higher duty cycle for the same environmental and shelter conditions. Fig. 10 shows LGCY and RH-U results for interior temperature in a Base-X 305 equipped with a DCAC. With the exception of two brief periods the DCAC is always running in the LGCY variant.

Figure 10: Thermal behavior of a Base-X 305 shelter equipped with a DCAC under LGCY and RH-U variants in the baseline grid configuration.

We point out two observations from these results. The first is the overall upward temperature bias in RH-U relative to LGCY. In the Base-X 305 with B0014 ECU shown in Fig. 8, the mean RH-U temperature is 1.2 F higher than the mean LGCY temperature. This difference rises to 5.8 F in the Base-X 305 with DCAC shown in Fig. 10. This is consistent with our thermal model, which recognizes that more energy—and more fuel—are required to maintain lower shelter interior temperatures.

The second, seemingly contrary, observation is that an optimally scheduled ECU will often initiate cooling well before approaching the high temperature limit. We draw two conclusions from this observation. First, the model elects to use currently available energy to do work now rather than store the energy in the battery to do work later. We discuss storage utilization further in Section 7.4 and Section 9.3. Finally, we conclude that the RH-U model validates our premise that time-shifting ECU operation can be employed to shape demand and lower overall overall fuel consumption.

As discussed in Section 5.2, evaluation of RH-U requires an assessment of the frequency and magnitude of temperature violations that occur due to differences between forecasted and actual environmental conditions. We observe only 20 minutes of temperature violation over the 90 shelter-hours modeled, resulting from ten instances in which the high temperature limit was breached.

7.3. Generator Operation

Analysis of generator operation provides deeper insights on the origin of fuel savings achieved through optimal ECU management. Fig. 11 displays the number of running generators in each period for the LGCY and RH-U models. Permitting optimal scheduling of both ECUs and generators provides our RH-U model the freedom to provision the most efficient generator mix capable of fulfilling demand.

Each model is encumbered with specific limitations, granted various optimization freedoms, and permitted a particular horizon visibility. These factors affect *how* it
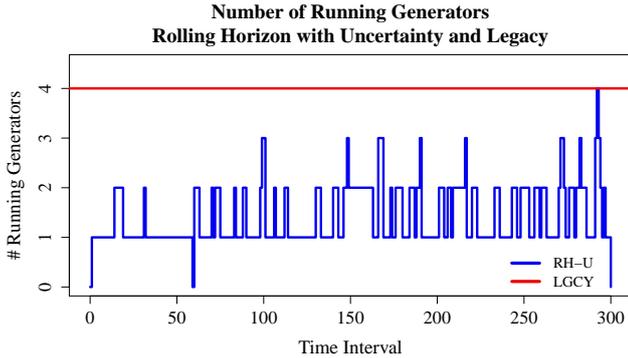
Figure 11: Number of running generators in each period for RH-U and LGCY in the baseline grid configuration.

Figure 12: Battery level for each model variant in the baseline grid configuration.

generates, stores, and utilizes power for temperature control. Because every model must achieve the same result of removing sufficient thermal energy from all shelters to maintain the desired temperature, however, the total amount of energy delivered to the loads is approximately equal for all variants. Given this requirement, RH-U and RH-PFK first reduce fuel consumption by provisioning fewer generators to deliver the total required energy over the course of our optimization period. The fuel savings from fewer running generators are compounded by the fact that each running generator must operate at higher—and more fuel efficient—load factors to deliver the same total energy.

7.4. Energy Storage

Battery level in the baseline grid configuration for each storage-capable model is shown in Fig. 12. We make two observations from this information. First, battery utilization is low for all variants despite our generously simplified battery model. At no time is more than 10% of our total 42 kWh battery capacity employed by any model variant. This is consistent with [15], who find diminishing returns from energy storage as grid design progresses from spot generation to a microgrid.

Our second observation is that the PFK-SOM model, despite having battery storage as its only avenue for optimization, makes very little use of available storage capability. This indicates that energy storage alone, without a concurrent ability to control electrical production or loads, offers limited benefit in our baseline grid.

8. Baseline Configuration Summary

Our suite of model variants evaluates baseline grid performance by using LGCY operation as an upper bound and perfect future knowledge, full management (PFK-FM) as a theoretical lower bound on fuel consumption. Intermediate variants offer insight on efficiency gains that may be achieved under various optimization opportunities and limitations on knowledge of future conditions.

In particular, the results for RH-U suggest the potential for computationally feasible optimal scheduling of
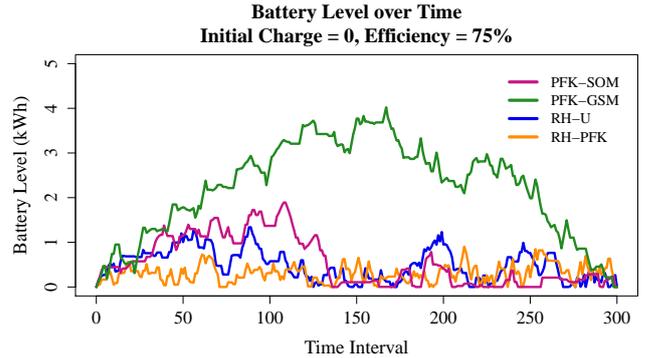
ECUs, generators, and storage devices to reduce fuel consumption relative to existing "always on" spot generation arrangements by as much as 28% while maintaining temperatures within specification and remaining tolerant of uncertainty in any remaining unmanaged loads.

9. Sensitivity Analysis

We continue our analysis of the configuration presented in Section 6 by conducting sensitivity analysis to evaluate the effect that changes to generator configuration, thermal and environmental parameters, storage characteristics, and unmanaged demand have on fuel consumption.

9.1. Generator Configuration

This section varies two aspects of the generator configuration: generator mix and the generator agility.

9.1.1. Generator Mix

Our baseline grid parameters dictate that the maximum electrical output demanded of the generators in any period is 56.23 kW[8], well below our total generation capacity of 110 kW. Fig. 13 shows the impact on fuel efficiency as we constrain the mix of generators available to our models.

We draw attention to three features of Fig. 13:

1. LGCY fuel consumption converges to our optimized fuel consumption as generation capacity approaches 60 kW, the minimum required to simultaneously supply all loads. By this point all running generators are at high load factors and within the upper portion of the generator fuel efficiency curve.

2. Below 60 kW generation capacity, unmanaged load may exceed production and LGCY becomes infeasible. Through optimal management of storage and remaining generators, PFK-GSM remains feasible down

---

[8]1 × 13 kW ECU + 5 × 4.5 kW ECU + 2 × 1.6 kW ECU + 1 × 8.5 kW ECU + 115% × 7.85kW unmanaged demand − 0 kW renewables
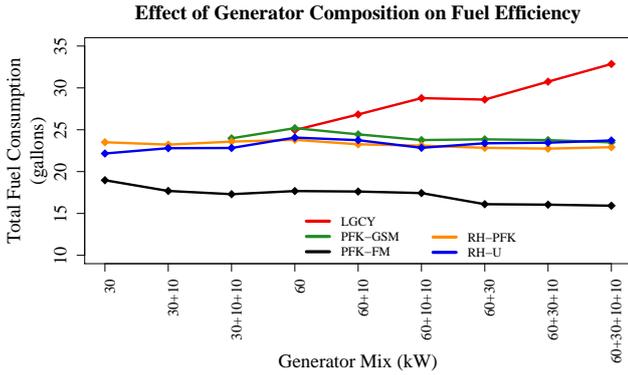
Figure 13: Effect of generator composition on fuel efficiency.

Figure 14: Effect of thermal model intercept on fuel efficiency.

Table 6: Comparison of LGCY and RH-U fuel consumption with changing environmental conditions.

Effect of Changing Environment on Fuel Consumption			
Thermal Intercept Scaling Factor	LGCY Fuel Consumption [gallons]	RH-U Fuel Consumption [gallons]	RH-U Reduction vs. LGCY [%]
0.6	21.64	7.99	63.1
0.7	24.02	10.59	55.9
0.8	26.76	15.05	43.8
0.9	29.84	19.69	34.0
1.0	32.90	23.60	28.3
1.1	35.52	27.83	21.7

to 50 kW of total generation capacity. By optimally managing generators, storage, *and* loads, RH-PFK and RH-U remain feasible and capable of supporting the grid under these particular environmental conditions with only 30 kW of total electrical production.

3. A single 60 kW generator uses slightly more fuel than its optimized 30+10+10 kW neighbor. While a 60 kW generator is the most efficient means of fulfilling the 56 kW peak demand, in practice a cluster of smaller generators may offer better aggregate efficiency for actual grid demand profiles.

Note that optimal scheduling provides the greatest improvements to fuel efficiency when the existing grid suffers from overgeneration, and diminishes to near-zero as the grid becomes ideally sized for the expected load. Our chosen baseline parameters serendipitously result in a maximum possible load that lies just within the capacity of the 60 kW generator, providing the LGCY model a better representation here than we would, on average, expect to see under a wider range of circumstances.

Further investigation into the ability of optimal scheduling to extend grid capability by multiplexing, or time-sharing generator output to serve collective loads in excess of net production capacity, is deferred to future studies.

9.1.2. Generator Agility

Recall that generators typically have required run\rest times in order to avoid equipment damage. More agile generators—those with shorter run and rest times—reduce optimization constraints and presumably offer the potential for greater fuel efficiency. Our baseline configuration sets run and rest times to five minutes, and our analysis reveals no significant changes to fuel efficiency as we run four of our model variants with run\rest times varying from 0 to 20 minutes, though the utilization of various generators by RH-U does vary with the run\rest time [18].

9.2. Thermal Conditions

We consider two modifications to thermal conditions: environmental changes, and changes within the shelter.

9.2.1. Environmental Influence

We implement changes in environmental conditions by adjusting the intercept value of our thermal model, with larger values corresponding to warmer exterior conditions and greater cooling requirements. Fig. 14 displays the results of running our baseline configuration with thermal intercept for each shelter scaled between 60% and 110% of its baseline values.

At scaling factors below 0.6 the Base-X 305 billeting shelters require heating and become infeasible in our current cooling-only model. At factors above 1.1 thermal burden exceeds the capacity of the DCACs and none of the variants are able to maintain the temperature of these shelters below the high limit.

Between these two levels we can see in Fig. 14 that differences in fuel consumption between LGCY and our optimized variants narrow as thermal burden increases. Table 6 details this relationship between LGCY and RH-U fuel consumption.

Increased thermal burden imposes two constraints upon ECUs. First, they must operate more *on average* to remove heat added throughout the optimization horizon and maintain shelter temperature within specifications. Second, interior temperatures rise faster and limit the length of time that an ECU may remain idle before a temperature limit is reached. These influences serve to limit time-
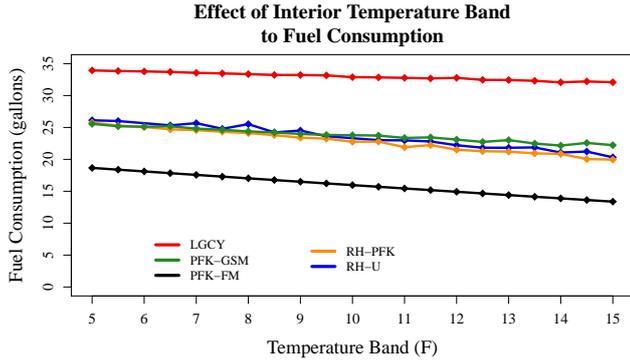
Figure 15: Effect of interior temperature band on fuel efficiency. Minimum interior temperature is held at 70 F while maximum interior temperature varies from 75 F to 85 F.
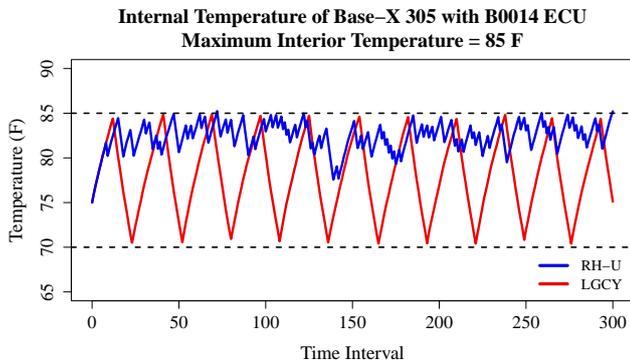
Figure 16: Interior temperature of a Base-X 305 shelter served by B0014 ECU with 70 F to 85 F temperature limits.

Figure 17: Interior temperature of a Base-X 305 shelter served by DCAC with 70 F to 85 F temperature limits.

shifting freedom and result in diminishing optimization advantages as load duty cycle increases.

9.2.2. Shelter Thermal Limits

Interior temperature limits are selected for personnel comfort and equipment safety and reliability. We evaluate the effect that changes to these limits have on fuel efficiency by maintaining a low limit of 70 F and varying our high limit from 75 F to 85 F. Results are displayed in Fig. 15, where we see fuel consumption declining as the distance between low and high temperature limits increases. These improvements are attributable to the increasing upper limit of our temperature band rather than the distance between high and low limits. Our optimization models require a sufficiently large temperature band to prevent infeasibilities in successive periods, but beyond this threshold there is no significant effect from a larger band. As seen in Figures 16 and 17, when provided the freedom to operate in a wide band the optimally scheduled ECUs elect to operate exclusively near the upper, more fuel efficient, limit.

9.3. Storage Utilization

Storage utilization for our model variants using the baseline 42 kWh battery with 75% efficiency is shown in

Section 7.4. Our sensitivity analysis explores the impact of changes to battery efficiency and capacity. We summarize our observations here; full results appear in [18].

9.3.1. Battery Efficiency

Executing the model with battery efficiency varying from 75% to 100%, we observe that the best integer solution for higher efficiencies improves upon the best theoretically possible solution of lower efficiencies, confirming a relationship between efficiency and fuel consumption. The practical impact is small in the configuration considered, suggesting that we would see, at most, a 3.6% reduction in fuel use if technological advances placed lossless storage options at our disposal.

9.3.2. Battery Capacity

Changes to battery capacity affect our storage-enabled model variants in two ways. First, additional capacity permits a larger amount of energy to be stored for use in future periods. Additionally, our model computes maximum battery charge and discharge rates as linear functions of battery capacity. Doubling capacity also doubles the *rate* at which energy can be placed into or removed from the battery.

We determine the impact of these joint effects on fuel consumption by varying battery capacity from 0 to 80 kWh under the RH-U variant. We observe that having additional capacity and higher charge\discharge rates offers no discernible benefit to an optimally scheduled system in our modeled configuration; in fact, the best possible solution for some battery capacities is marginally worse than the best possible solution for a lower battery capacity. We attribute this to our choice of absolute and relative optimality gaps and to the rolling horizon methodology that makes early decisions before all information is known.

We conclude that storage is a minor contributor to fuel efficiency under the conditions we have modeled. We encourage further research that extends this methodology to evaluation of additional grid configurations and performs multi-factor designed experiments to isolate the effects of

battery capacity, efficiency, and charge/discharge rates on fuel efficiency.

9.4. Variations in Unmanaged Demand and Renewable Production

Variations in unmanaged demand or renewable generation of up to 20% from forecasted levels ($var_a, var_u \leq 20\%$) do not have any significant effect on fuel consumption in the RH-U variant. At our forecasted value for unmanaged demand of 7.85 kW in each period, a 20% variation results in no more than ± 1.6 kW difference between forecasted planning and actual execution. This is small in relation to total load and sufficiently explains our observations.

We propose further research to evaluate environments with greater variations in unmanaged demand or unmanaged demand that is a larger proportion of overall demand. Additionally, we recommend consideration of robust demand handling mechanisms that would, for example, perform priority-based cancellation and rescheduling of time-shiftable events to accommodate unmanaged demand variability without over-provisioning generators.

9.5. Summary

Analysis for our modeled configuration shows that the fuel efficiency of optimally scheduled systems relative to existing "always-on" systems is sensitive to (1) the excess generation capacity of the legacy system, (2) load duty cycles due to thermal burden on the shelter and ECU system, and (3) shelter interior temperature limits. Our results are not sensitive to storage capacity, storage efficiency, or generator run\rest times.

10. Conclusion

Expeditionary energy is enormously costly for the US military, both in terms of money and lives. A substantial portion of this energy is used in unmanaged, inefficient systems to satisfy the heating and cooling needs of personnel and equipment. This paper has presented an optimization-based methodology for improving the efficiency of expeditionary energy grids through active load scheduling that enables superior provisioning and operation of tactical generators. Our analysis indicates that significant fuel savings can be achieved with minimal degradation in performance. For a grid configuration based on an actual tactical power system fielded in Afghanistan, our model obtains a 28% reduction in fuel while maintaining structure temperatures within the nominal range during 97% of the optimization time horizon.

Extending this model to include additional time-shiftable expeditionary loads, such as refrigeration and potable water production, would broaden the optimization potential. We expect this would yield further efficiencies.

Acknowledgements

Appendix: Detailed Model Run Times

Optimization was performed in GAMS running in Windows 7 on a Dell Precision T7500 workstation equipped with dual Intel Xeon X5675 3.06 GHz processors and 64 gigabytes (GBs) of memory. Problem sizes and solution times are listed in Table 7. Our stopping conditions included a relative optimality gap of 4% and an absolute optimality gap of 0.15 gallons. Our rolling horizon implementations included 300 2-minute intervals (10 hours total), with 20 horizons of 30 minutes each.

Table 7: Solution times and problem dimensions for the baseline configuration.

Optimization Dimensions and Solution Times					
			Variables		
Variant	Time	Constraints	Total	Binary	SO
LGCY	< 2 sec	2,408	6,897	-	
PFK-SOM	< 10 sec	3,000	8,160	-	
PFK-GSM	< 3 min	18,596	14,437	3,604	1,
RH-PFK	8 to 19 min[†]	3,711	2,527	1,183	1
RH-U	12 to 20 min[†]	3,711	2,527	1,183	1
RMIP	< 10 sec	37,461	24,005	-	

References

[1] M. Schwartz, K. Blakely, R. O'Rourke, Department of Defense Energy initiatives: Background and issues for Congress, CRS Report R42558, Congressional Research Service, Washington, DC (Jun. 2012).

[2] 10 u.s. code 2924(5).

[3] Office of the Assistant Secretary of Defense (Energy, Installations, and Environment), Department of Defense annual energy management report for fiscal year 2014, Report, Department of Defense, Washington, DC (May 2015).

[4] Office of the Assistant Secretary of Defense (Energy, Installations, and Environment), Department of Defense annual energy management report for fiscal year 2013, Report, Department of Defense, Washington, DC (Oct. 2014).

[5] A. M. Andrews, W. Bryzik, R. Carlin, J. M. Feigley, W. E. Harrison III, D. J. Katz, J. Y. Rodriquez, R. L. Snead, J. C. Sommerer, J. T. Tozzi, G. E. Webber, W. Weldon, J. Wolbarsht, Future fuels, Tech. Rep. NRAC 06-1, Naval Research Advisory Committee, Arlington, VA (Apr. 2006).

[6] T. C. Moore, B. H. Newell, J. L. Alderman, R. Dickson, D. Nolan, J. W. Barnett, Report of the Afghanistan Marine energy assessment team, Tech. rep. (Jan. 2011).

[7] Office of the Commandant of the Marine Corps, Washington, DC, United States Marine Corps Expeditionary Energy Strategy Implementation Planning Guidance (Feb. 2011).

[8] M. Gillman, W. M. Singleton, R. A. Wilson, W. Cotta, J. Donnal, J. Paris, S. Leeb, Accounting for every kilowatt, Defense AT&L XLIII (5) (2014) 44–49.

[9] U.S. Government Accountability Office, Defense management: Steps taken to better manage fuel demand but additional information sharing mechanisms are needed, GAO Report GAO-12-619, U.S. Government Accountability Office, Washington, DC (Jun. 2012).

[10] U.S. House. 111th Congress, 1st Session. (2009, Mar 3), Department of Defense Fuel Demand Management at Forward-Deployed Locations and Operational Energy Initiatives.
URL http://www.gpo.gov/fdsys/pkg/CHRG-111hhrg51161/pdf/CHRG-111hhrg51161.pdf

[11] D. S. Eady, S. B. Siegel, R. S. Bell, S. H. Dicke, Sustain the mission project: Casualty factors for fuel and water resupply convoys, Final Technical Report CTC-CR-2009-163, Army Environmental Policy Institute, Arlington, VA (Sep. 2009).

[12] S. B. Siegel, S. Bell, S. Dicke, P. Arbuckle, Sustain the mission project: Energy and water costing methodology and decision support tool, Final technical report, Army Environmental Policy Institute, Arlington, VA (Mar. 2008).

[13] U.S. Dept. of the Air Force, Washington, DC, Guide to Contingency Electrical Power System Installation, Air Force Handbook 10-222, vol 5 Edition (Sep. 2008).

[14] P. Bulanow, P. Tabler, S. Charchan, Expeditionary energy assessment environmental control unit alternatives study, Final report, Quantico, VA (Jul. 2011).

[15] S. B. Van Broekhoven, E. Shields, S. V. T. Nguyen, E. R. Limpaecher, C. M. Lamb, Tactical power systems study , Technical Report 1181, Lincoln Laboratory, Massachusetts Institute of Technology, Lexington, MA (May 2014).

[16] G. Dogum, Village stability operations VS-platform: Power site surveys, Trip report, U.S. Army Research, Development, and Engineering Command (RDECOM) Field Assistance in Science and Technology Center (FAST-C) (Jul. 2012).

[17] C. Bolton, private communication (Jul. 2015).

[18] J. G. Sprague, Optimal scheduling of deferrable electric loads in expeditionary power grids, Master's thesis, Ops. Research Dept., Naval Postgraduate School, Monterey, CA (2015).

[19] E. Anderson, M. Antkowiak, R. Butt, J. Davis, J. Dean, M. Hillesheim, E. Hotchkiss, R. Hunsberger, A. Kandt, J. Lund, K. Massey, R. Robichaud, B. Stafford, C. Visser, Broad overview of energy efficiency and renewable energy opportunities for Department of Defense installations, Tech Report NREL/TP-7A20-50172, National Renewable Energy Laboratory (NREL), Golden, CO (Aug. 2011). doi:10.2172/1023698.
URL http://www.osti.gov/servlets/purl/1023698-6alCol/

[20] National Research Council, Force multiplying technologies for logistics support to military operations, Tech. rep., The National Academies, Washington, DC (Dec. 2014).

[21] H. Bouaicha, H. Dallagi, E. Craparo, S. Nejim, Economic scheduling of a hybrid microgrid based on weather forecasts, in: 2017 International Conference on Advanced Systems and Electric Technologies (IC-ASET), 2017, pp. 110–117. doi:10.1109/ASET.2017.7983675.

[22] N. A. Ulmer, Optimizing microgrid architecture on department of defense installations, Master's thesis, Ops. Research Dept., Naval Postgraduate School, Monterey, CA (Sep. 2014).

[23] A. M. Newman, Energy resource planning tool for the Office of Naval Research, presented at Naval Postgraduate School, Monterey, CA, 2015.

[24] M. Sadiqi, A. Pahwa, R. D. Miller, Basic design and cost optimization of a hybrid power system for rural communities in Afghanistan, in: North American Power Symposium (NAPS), Champaign, IL, 2012, pp. 1–6. doi:10.1109/NAPS.2012.6336333.

[25] J. S. Vardakas, N. Zorba, C. V. Verikoukis, A survey on demand response programs in smart grids: Pricing methods and optimization algorithms, Communications Surveys & Tutorials, IEEE 17 (1) (2015) 152–178. doi:10.1109/COMST.2014.2341586.

[26] Energy Storage Association, Spinning Reserve (n.d.) [cited 8/4/2015].
URL http://energystorage.org/energy-storage/technology-applications/spinning-reserve

[27] M. C. Vlot, J. D. Knigge, J. G. Slootweg, Economical regulation power through load shifting with smart energy appliances, IEEE Transactions on Smart Grid 4 (3) (2013) 1705–1712. doi:10.1109/TSG.2013.2257889.
URL http://ieeexplore.ieee.org/xpls/abs_all.jsp?arnumber=6513322

[28] D. T. Nguyen, L. B. Le, Optimal bidding strategy for microgrids considering renewable energy and building thermal dynamics, IEEE Transactions on Smart Grid 5 (4) (2014) 1608–1620. doi:10.1109/TSG.2014.2313612.
URL http://ieeexplore.ieee.org/xpls/abs_all.jsp?arnumber=6839078

[29] P. Tarasak, C. C. Chai, Y. S. Kwok, Demand bidding program and Its application in hotel energy management, IEEE Transactions on Smart Grid 5 (2) (2014) 821–828.
URL http://ieeexplore.ieee.org/xpls/abs_all.jsp?arnumber=6732972

[30] Southern California Edison, Demand Bidding Program.
URL https://www.sce.com/wps/wcm/connect/96702c0a-c759-4efe-b302-f874e4407c32/090217_Demand_Bidding_Fact_Sheet.pdf?MOD=AJPERES

[31] Flexible operation of active distribution network using integrated smart buildings with heating, ventilation and airconditioning systems, Applied Energy (2018) 181,196.

[32] Demand side management of photovoltaic-battery hybrid system, Applied Energy (2015) 294,304.

[33] Energy management and load shaping for commercial microgrids coupled with flexible building environment control, Journal of Energy Storage (2018) 61,75.

[34] G. Wilkenfeld, A national demand management strategy for small airconditioners: The role of the national appliance and equipment energy efficiency program, National Appliance and Equipment Energy Efficiency Committee Report 2004/22 (November 2004).

[35] I. Koutsopoulos, L. Tassiulas, Challenges in demand load control for the smart grid, IEEE Network 25 (5) (2011) 16–21. doi:10.1109/MNET.2011.6033031.
URL http://ieeexplore.ieee.org/xpls/abs_all.jsp?arnumber=6033031

[36] E. Thompson, Army successfully demonstrates tactical operations smart grid (Oct. 2012).
URL http://www.army.mil/article/88440/

[37] J. Vavrin, Power and energy considerations at forward operating bases (FOBs), presented at the NDIA Environment, Energy Security & Sustainability (E2S2) Symposium & Exhibition, Denver, CO, 2010.

[38] J. Silvente, G. M. Kopanos, E. N. Pistikopoulos, A. Espua, A rolling horizon optimization framework for the simultaneous energy supply and demand planning in microgrids, Applied Energy 155 (2015) 485 – 501. doi:https://doi.org/10.1016/j.apenergy.2015.05.090.
URL http://www.sciencedirect.com/science/article/pii/S0306261915007230

[39] U.S. Dept. of the Army, Washington, DC, Engineer Prime Power Operations, TM 3-34.45 Edition (Aug. 2013).

[40] B. Bloodworth, COP Chak DC trip report, Trip report, U.S. Army Corps of Engineers, Champaign, IL (Nov. 2011).

[41] B. Bloodworth, COP Nerkh trip report, Trip report, U.S. Army Corps of Engineers, Champaign, IL (Nov. 2011).

[42] W. M. Solis, Defense management: DOD needs to increase attention on fuel demand management at forward-deployed locations, GAO Report GAO-09-300, U.S. Government Accountability Office, Washington, DC (Feb. 2009).

[43] J. Whitmore, Intelligent Power Management Distribution Systems (IPMDS), presented at the 2011 Joint Service Power Expo, Myrtle Beach, SC, 2011.
URL http://www.dtic.mil/ndia/2011power/Session2_12093_Whitmore.pdf

[44] Large power sources (n.d.)., accessed Aug. 18, 2015 [cited 8/2/2015].

URL `http://www.peocscss.army.mil/PdDLPS.html`

[45] L. Murphy, Creating energy efficiency on the battlefield, White paper, DRASH Systems, Accessed Aug. 5, 2015 ((n.d.)).
URL `http://www.drash.com/userfiles/File/White%20Paper/IPT%20White%20Paper.pdf`

[46] J. Andrews, N. Jelley, Energy Science: Principles, Technologies, and Impacts, Oxford Univ. Press, Oxford, UK, 2013.

[47] Department of the Air Force, Washington, DC, Bare Base Assests, Air Force Handbook 10-222, Volume 2 Edition (Feb. 2012).

[48] Program Manager, Expeditionary Power Systems, Environmental Control Equipment (ECE), in: Environmental Control and Power Sources Equipment, no. TM 12359A-OD, Ch. 4, U.S. Marine Corps Systems Command, Quantico, VA, 2011, Ch. 4.
URL `http://www.marcorsyscom.marines.mil/Portals/105/pdmeps/docs/ECE/TM%2012359A-OD-C%20JUNE2011%20ECU.pdf`

[49] NPR Staff, Among the costs of war: Billions a year in A.C.? (Jun. 2011).
URL `http://www.npr.org/2011/06/25/137414737/among-the-costs-of-war-20b-in-air-conditioning`

[50] U.S. Army Natick Soldier Research, Development, and Engineering Center, Commanders' Smartbook Equipment Catalog, Natick, MA (Apr. 2013).

[51] Joint Committee OnTactical Shelters (JOCOTAS), Department of Defense Standard Family of Tactical Shelters (Rigid/Soft/Hybrid), Natick, MA (May 2012).

[52] U.S. Army Natick Soldier Research, Development and Engineering Center, Fabric structures team technology update, presented at the 7th Bi-Annual DOD JOCOTAS Meeting with Rigid Soft Wall Shelter Industry and Indoor & Outdoor Exhibition, Natick, MA, 2011.

[53] W. M. Solis, Increased attention on fuel demand management at DOD's forward-deployed locations could reduce operational risks and costs, Testimony Before the Subcommittee on Readiness, Committee on the Armed Services, House of Representatives GAO-09-388T, Government Accountability Office, Washington, DC (Mar. 2009).

[54] U.S. Marine Corps Systems Command, Quantico, VA, Operation/Maintenance Manual for Mobile Electric Power Distribution System Replacement (MEPDIS-R), TM 6110-OI-1 Edition (Feb. 2012).

[55] U.S. Army Headquarters, Washington, DC, Operator and Field Maintenance Manual for Power Distribution Illumination Systems, Electrical (PDISE), TM 9-6150-226-13 Edition (Apr. 2012).

[56] J. Antonetti, Low-sulfur diesel fuel (DL)-2 and jet propellant (JP)-8 fuel consumption test Advanced Medium Mobile Power Sources (AMMPS), Tech. Rep. ATC-11590, Fort Belvoir, VA (Aug. 2014).

[57] E. Craparo, M. Karatas, D. I. Singham, A robust optimization approach to hybrid microgrid operation using ensemble weather forecasts, Applied Energy 201 (2017) 135 – 147. `doi:https://doi.org/10.1016/j.apenergy.2017.05.068`.
URL `http://www.sciencedirect.com/science/article/pii/S0306261917305172`

[58] E. Shields, B. H. Newell, Current power and energy requirements of forward deployed USMC locations, presented at the NDIA Environment, Energy Security & Sustainability (E2S2) Symposium & Exhibition, May 22, 2012.

[59] B. H. Newell, E. B. Shields, USMC expeditionary energy office report on expeditionary energy data collection within Regional Command Southwest, Afghanistan, Tech. rep., USMC Expeditionary Energy Office (Sep. 2012).